AGU PUBLICATIONS

Water Resources Research

RESEARCH ARTICLE
10.1002/2016WR020105

Hindered erosion: The biological mediation of noncohesive sediment behavior

X. D. Chen[1], C. K. Zhang[1], D. M. Paterson[2], C. E. L. Thompson[3], I. H. Townend[4], Z. Gong[1], Z. Zhou[1], and Q. Feng[5,6]

[1]College of Harbor, Coastal and Offshore Engineering, Hohai University, Nanjing, China, [2]Sediment Ecology Research Group, Scottish Oceans Institute, School of Biology, University of St Andrews, Fife, UK, [3]School of Ocean and Earth Science, National Oceanography Centre, Southampton, Hampshire, UK, [4]University of Southampton, Southampton, UK, [5]Key Laboratory for Integrated Regulation and Resources Exploitation on Shallow Lakes of Ministry of Education, Hohai University, Nanjing, China, [6]College of Environment, Hohai University, Nanjing, China

Key Points:
- Spatial and temporal changes in the concentration of EPS in the sediment are quantified over a depth profile
- The effect of EPS in hindering the erosion of both surface and underlying sediment is determined alongside bacterial development
- A conceptual erosion framework is proposed for biosedimentary system recognizing the variation from the traditional abiotic approach

Supporting Information:
- Supporting Information S1

Correspondence to:
C. K. Zhang,
ckzhang@hhu.edu.cn;
Q. Feng,
xiaofq@hhu.edu.cn

Citation:
Chen, X. D., C. K. Zhang, D. M. Paterson, C. E. L. Thompson, I. H. Townend, Z. Gong, Z. Zhou, and Q. Feng (2017), Hindered erosion: The biological mediation of noncohesive sediment behavior, *Water Resour. Res.*, *53*, doi:10.1002/2016WR020105.

Received 10 NOV 2016
Accepted 15 MAY 2017
Accepted article online 22 MAY 2017

Abstract Extracellular polymeric substances (EPS) are ubiquitous on tidal flats but their impact on sediment erosion has not been fully understood. Laboratory-controlled sediment beds were incubated with *Bacillus subtilis* for 5, 10, 16, and 22 days before the erosion experiments, to study the temporal and spatial variations in sediment stability caused by the bacterial secreted EPS. We found the biosedimentary systems showed different erosional behavior related to biofilm maturity and EPS distribution. In the first stage (5 days), the biosedimentary bed was more easily eroded than the clean sediment. With increasing growth period, bound EPS became more widely distributed over the vertical profile resulting in bed stabilization. After 22 days, the bound EPS was highly concentrated within a surface biofilm, but a relatively high content also extended to a depth of 5 mm and then decayed sharply with depth. The biofilm increased the critical shear stress of the bed and furthermore, it enabled the bed to withstand threshold conditions for an increased period of time as the biofilm degraded before eroding. After the loss of biofilm protection, the high EPS content in the sublayers continued to stabilize the sediment (hindered erosion) by binding individual grains, as visualized by electron microscopy. Consequently, the bed strength did not immediately revert to the abiotic condition but progressively adjusted, reflecting the depth profile of the EPS. Our experiments highlight the need to treat the EPS-sediment conditioning as a bed-age associated and depth-dependent variable that should be included in the next generation of sediment transport models.

Plain Language Summary Sedimentology and geomorphology have traditionally been seen as fields in which physical and chemical processes dominate. However, microbial communities should never be bystanders, because they suffuse all sedimentary environments on earth. Under hydrodynamic forces, they take part in an impressive range of sediment processes and thus exercising a formative influence on coastal evolutions. Bio-sediments exhibit more complex characteristics than abiotic systems, and lead to different modelling methods compared to those in traditional settings. For instance, the thresholds for sediment initiation and subsequent erosion rates are no longer solely related to particle properties (e.g., particle size, the most widely used), but mediated by glue-like extracellular polymeric substances (EPS) secreted by microbes. From this point of view, it is easy to understand why sediments in field observations behave differently from predictions, usually appearing considerably strengthened. Our results indicate that the EPS mediation in sediment stability may vary with the rhythms of microbial growth, and re-profile the sediment stability during different stages of cementing processes. A conceptual framework for sediment erosion is hence put forward to transform traditional sediment system to EPS-sediment system.

1. Introduction

Understanding sediment dynamics has long been a critical issue for hydraulics researchers and engineers. The redistribution of sediments is recognized as central to a range of management strategies (e.g., channel dredging, tidal land reclamation, and coastal protection). Sediment movement is also of ecological and environmental concern since many pollutants and pathogens adhere to and are transported with cohesive

sediment in aquatic systems [*Craig et al*., 2001; *Droppo et al*., 2009; *Haag et al*., 2001]. Meanwhile, in biogeomorphological ecosystems such as mangroves, saltmarshes or river flood plains, the condition of vegetation is closely linked with bank stability, which in turn is related to sediment erosion and deposition processes [*Balke et al*., 2014]. Extensive research efforts have been devoted to understanding, predicting and managing sediment behavior in aquatic environments, often based on laboratory experiments using well-sorted grains and sediments cleaned of any microbial or organic "contamination" [*Paterson and Black*, 1999]. Relevant parameterizations for predicative models and management (e.g., threshold for erosion shear stress, bed roughness) are normally developed via empirical fitting from laboratory tests, and hence may not be applicable to the full range of natural environments [*Black et al*., 2002]. Nevertheless, an increasing number of studies report that microbial interactions with sediments play a significant role in the stabilization of the bed against erosive forces and subsequently affect sediment transport [*Malarkey et al*., 2015].

In natural rivers, mudflats or any other areas with rich natural microbial communities, biogenic effects on sediment dynamics and movement characteristics cannot be considered as negligible [*Grant and Gust*, 1987; *Paterson*, 1989; *Stone et al*., 2008; *Volk et al*., 2016]. This phenomenon of "biostabilization" or "biogenic stabilization" and is defined as a decrease in sediment erodibility caused by biological action [*Paterson and Daborn*, 1991]. An important mechanism of biogenic stabilization is through the production of extracellular polymeric substances (EPS) by sediment-inhabiting organisms. EPS is a generic term that describes all long chain molecules that can be produced by a wide range of organisms from bacteria to macrofauna. Perhaps the most influential EPS in biostabilization are the polymers secreted by the microbial communities inhabiting the sediment. The organic molecules can cover and cohere sediment particles, hence increasing sediment stability and resistance to hydrodynamic forcing [*Paterson*, 1989]. Even for largely noncohesive sandy systems, very small amounts of EPS are sufficient to produce a substantial change in bed form type and dimensions [*Hagadorn and Mcdowell*, 2012; *Parsons et al*., 2016] and bed form growth rates [*Malarkey et al*., 2015]. In addition, recent studies have revealed that biofilms interact with the local flow structure [*Graba et al*., 2013; *Vignaga et al*., 2013]. In fact, examining the role of biocohesive forces to improve our understanding of natural sediment dynamics is increasingly being highlighted as a priority by sedimentologists and geomorphologists [*Le Hir et al*., 2007; *Noffke and Paterson*, 2008; *Passarelli et al*., 2014; *Schindler et al*., 2015; *Zhou et al*., 2016].

Existing studies of biostabilization have mostly focused on "surface phenomenon" reflected by the increase in the critical shear stress for erosion [*Fagherazzi et al*., 2013; *Taylor and Paterson*, 1998; *Tolhurst et al*., 2006]. However, biogenic stabilization is not necessarily confined to the presence of a surface biofilm and its effects. EPS may penetrate the surface of the sediment matrix and establish a vertical profile, with consequent effects not only on critical erosion threshold but erosion rates. There have been very few studies dealing with this phenomenon although this would certainly provide greater understanding of the erosion process and promote improved prediction of the sediment transport on larger spatial scales for morphological calculations [*Gerbersdorf et al*., 2005]. Although relatively small amounts of EPS have recently been reported to be important in predicting bed form behavior in sandy system [*Malarkey et al*., 2015; *Parsons et al*., 2016], the vertical distribution was assumed to be homogeneous, and also a proxy for natural EPS (e.g., xanthan gum) was used to provide biological cohesion. However, in intertidal systems, natural spatial and temporal variations of biogenic effects are the status quo. EPS produced by bacteria and microphytobenthos accumulate and decay in response to biological and temporal (diurnal, seasonal, annual) changes. Extreme weather conditions may regularly disrupt biosediment systems, which then reestablish during a calmer building period. Therefore, shifts occur between deposited sediments of relatively low organic content and later conditions where, after a period of calm, EPS accumulates and biostabilization becomes more influential. During this process, EPS may become distributed into the sediment matrix and it is important to know the natural development of the EPS profile through different growth periods. Consequently, the behavior of biogeomorphological ecosystems is strongly linked with the development of the biogenic matrix ranging from low EPS states (close to the clean sediment) to high-EPS states (where bioeffects become nonnegligible). Hence, the specific research questions to be addressed in this study are: (1) What depth of sediment is influenced by EPS? (2) How does this EPS affect sediment stability as reflected in different erosion processes? (3) How can we relate changes in sediment erosion patterns to the depth profile of EPS content? To address these questions, we conducted laboratory experiments to quantify microscale spatial and temporal changes in sediment stability and erosion patterns as influenced by EPS. Finally, a

conceptual framework was developed to examine microbial effects on fine sand, and the consequences of EPS mediation of noncohesive sediment erosion.

2. Materials and Methods

2.1. Experimental Setup

The experimental sediment was collected at Site SM89 from the lower intertidal zone of tidal flats in Yancheng, Jiangsu Province, China (Figure 1a). The Jiangsu coastal area (119°30′E–122°20′E, 31°30′N–35°15′N) in the South Yellow Sea comprises rich tidal flats sheltered by large radial sand ridges [*Zhang et al*., 2016]. Sediment was collected in the lower intertidal zone and was predominantly noncohesive fine grained and often reworked [*Xu et al*., 2016; *Zhang et al*., 1999]. In the summer, the sediment at Site 7 was usually covered with biofilms (Figure 1b).

The sampled sediment was sieved to remove the cohesive fraction (sieve 30 μm). The median grain diameter (D_{50}) after sieving was 108 μm (supporting information Figure S1 for the grain size distribution). The sediment was then washed with hydrogen peroxide to remove organisms and organic material. Six identical 20 L benthic chambers (290 mm diameter $\times$ 250 mm high) with rotating paddles were used in this study (Figure 2). The device is an improved version of the UMCES Gust Erosion Microcosm System (U-GEMS) [*Thomsen and Gust*, 2000] and Core Mini Flume (CMF) [*Thompson et al*., 2013], comprising a benthic device with flow capability used for determining sediment erosion thresholds. A small island was placed (150 mm in diameter) at the center of the test bed in order to: (1) limit the effect of the flow vortices, often produced in the central region of the flow field, affecting the center of the bed; (2) provide a more evenly distributed shear stress over the outer annular test region (assessed using a simplified model and three-dimensional Doppler Velocimetry (Vectrino Profiler, Nortek AS), see supporting information Figure S2 for more details). Spatial variations and boundary effects in the radial direction increased with the paddle revolutions per minute (rpm). One chamber (A) was used as a control in which the clean sediment was eroded in artificial

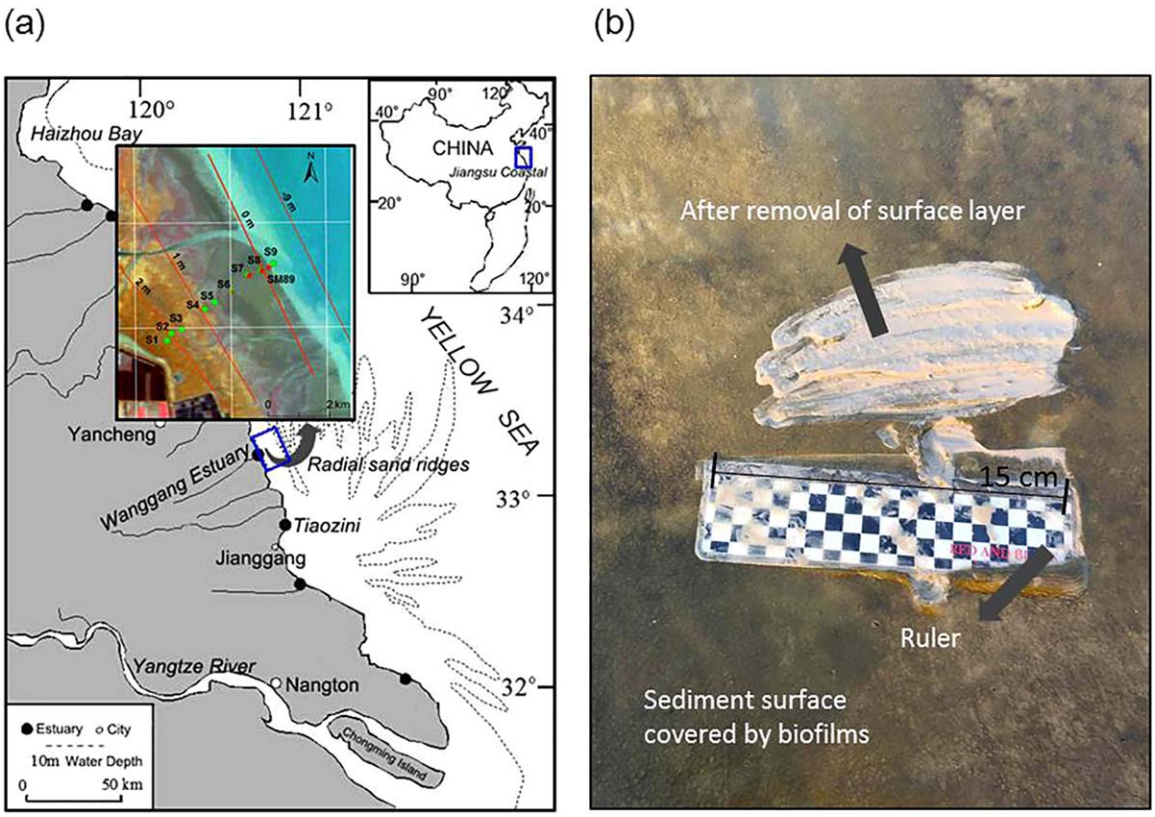

Figure 1. (a) Jiangsu coastal area and the location of the study sites, where Site S6-SM89 marks the transition to the lower intertidal zone. (b) Example of the surface sediment at Site S7 in June, 2016. Biofilms cover the sediment surface, which form extensive brown or golden-brown mats of microphytobenthos and bacteria.

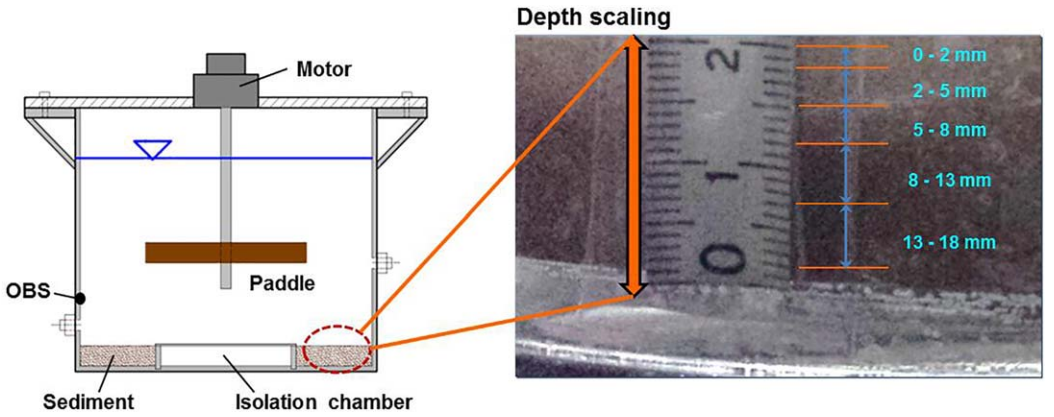

Figure 2. (left) Biosediment cultivation and erosion chamber and (right) sediment core samples indicating the five layers used in the analysis of the bed.

sea water (ASW, salinity of 23). "Biosedimentary" beds were developed from clean sediments by incubation of selected bacteria in ASW with added nutrients. Monitoring data from the offshore area in Jiangsu coastal zone were selected as the parameters for the environmental settings in this experiment. Incubation of the biosedimentary beds occurred under a constant bottom shear stress of 0.058 Pa which allowed the growth of biofilms and was lower than the critical shear stress to avoid the resuspension of sand grains. All the chambers were maintained at a temperature of 20 ± 2°C in ASW. The ASW containing abundant ($>10^7$ CFU/g) *Bacillus subtilis* (bacterial powder supplied by Guangzhou Weiyuan Biotechnology Co., Ltd) was added with a bulk medium phosphate buffer (pH 7.5). The substrate media consisted of: 0.2 g L^{-1} glucose (0.3 g glucose m^{-2} d^{-1}), 0.8 g L^{-1} CH_3COONa (1.1 g CH_3COONa m^{-2} d^{-1}), 0.05 g L^{-1} tryptone (0.075 g tryptone m^{-2} d^{-1}), and 0.05 g L^{-1} bacto-extract (0.075 g bacto-extract m^{-2} d^{-1}) [*Garny et al*., 2008]. The nutrient concentrations were increased over field values, to avoid nutrient limitation during growth under experimental conditions. Planktonic growth was limited by replacing the reactor volume with a fresh medium every 2–3 days. Biosediment beds were incubated for different growth periods (5, 10, 16, 22 days) in experimental chambers (B-E) after which erosion experiments were conducted. Chamber F contained an incubated biosedimentary system for 25 days and was used for the extraction of sediment samples (every 2–5 days).

2.2. Analytical Method

Sediment cores (50 mm in diameter) were taken from a different region in chamber F every 2–5 days, and sectioned into five layers (Figure 2, depth below surface: 0–2, 2–5, 5–8, 8–13, 13–18 mm) and used for analysis of EPS content and scanning electron microscopy (SEM, HITACHI S-3000N, 25 kV, freeze drying method was used for sample preparation) of sediment bed morphology.

The EPS extraction method was modified from Liang [*Liang et al*., 2010] and Li [*Li et al*., 2008], to improve extraction efficiency. The volatile suspended solids (VSS) in each sediment sample were measured in advance according to standard methods [*American Public Health Association* (*APHA*), 1998]. The EPS was extracted from 3 mL of fresh sediment which was placed in 50 mL centrifuge tubes with the addition of sterile deionized water (30 mL total volume). Tubes were then centrifuged (4000*g*, 10 min, 4°C) after which the supernatant was recentrifuged (13,200*g*, 20 min, 4°C) to ensure complete removal of the suspended solids. The resultant supernatant was then analyzed for colloidal EPS (C-EPS) content. The bottom sediments were resuspended in 30 mL of sterile deionized water and treated by ultrasound (ultrasonic bath, 40 W, 21 kHz, 2 min). After that, bound EPS (B-EPS) was extracted by adding 60 g/g VSS of cation exchange resin (CER) then oscillating the sample (500 rpm, 60 min, 4°C). The residual solids were removed by high speed centrifugation (10,000*g*) for 15 min and bound EPS was collected in the supernatant after filtering through a 0.45 μm filter membrane.

The EPS yields were represented as polysaccharides, protein, and humic acids; the main components of EPS [*Gao et al*., 2008]. A modification of the anthrone method [*Raunkjaer et al*., 1994] was applied for the measurement of polysaccharide content in EPS with glucose as the standard. The protein and humic content in

EPS were measured by the Lowry method [*Lowry et al*., 1951] using bovine serum albumin and humic acid as the respective standards.

2.3. Erosion Experiment Design

For the erosion experiments, the rotational speed of the paddles (and therefore applied bed-shear stress) was increased in stepwise time increments. When the threshold for erosion was exceeded, the time increments for each further stress increase were sufficient for the bed to reach equilibrium (erosion rate declines to zero) at the applied level of shear stress, *Paterson and Black* [1999]). An optical backscatter sensor (OBS-3+) located 7 cm above the bed surface was used to measure the real-time suspended sediment concentration (SSC) (the calibration of the OBS for the sand grains used in this study can be found in supporting information Figure S3). The monitoring range depends on sediment size, particle shape, and reflectivity. For the sediment used in this study, the maximum concentration was 60 kg/m^3 (3.5% by volume). The bottom shear stress for each rotating speed was determined using the Turbulent Kinetic Energy (TKE) method [*Al-Ragum et al*., 2014; *Pope et al*., 2006; *Stapleton and Huntley*, 1995]. A Vectrino Profiler (Nortek AS) was employed to obtain instantaneous velocity in three dimensions within an *xyz* coordinate system in order to calculate the TKE from turbulent velocity (details in supporting information Text S1).

3. Results and Discussion

3.1. EPS Distribution

The EPS concentrations in the surface layer of sediment in the test systems increased with time until reaching a stable state after approximately 20 days (Figure 3a). The EPS accumulation rate was initially low but increased rapidly over the first week before reaching equilibrium. The biofilm reached maturity after approximately 18 days of development. The content of the B-EPS in the first layer (0–2 mm) tended to reach equilibrium before the formation of mature biofilm (after about 10 days) (Figure 3b).

In biotechnology, many EPS polysaccharides have been explored for commercial applications in the food and cosmetic industries. For instance, xanthan gum has been widely used as a stabilizer, emulsifier or gel to improve cohesive strength and has commonly been selected as an EPS proxy to recreate the biocohesion of sediment as opposed to physical cohesion [*Parsons et al*., 2016]. The EPS polysaccharides seem to contribute considerably to the observed binding effects creating a gel-matrix structure, while proteins may promote the growth of microbes and enhance biofilm formation, with further positive effects on sediment stability [*Gerbersdorf and Wieprecht*, 2015]. There is also increasing evidence of the structural role of proteins, but their function appears to be highly dependent on the types of proteins present [*Flemming*, 2011; *Pennisi*, 2002].

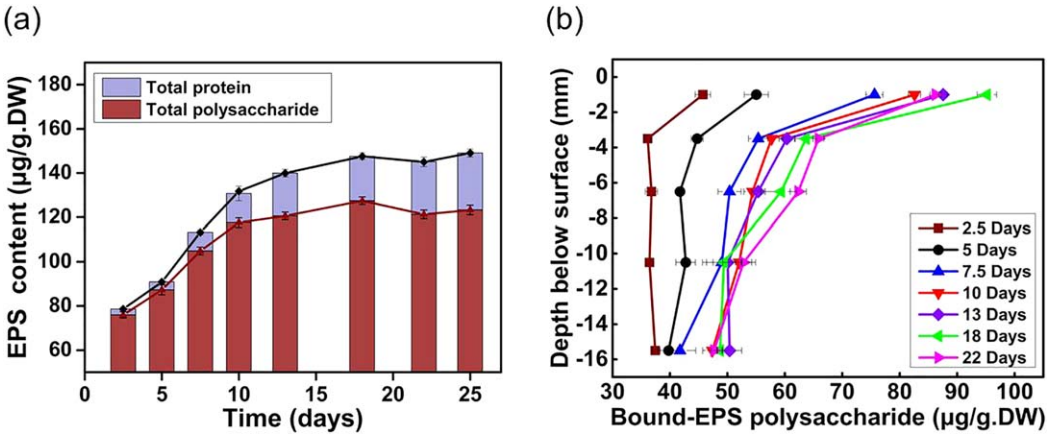

Figure 3. (a) Surficial EPS contents in the upper 2 mm layer (total polysaccharide and protein, no humic content observed) show the variation during the biofilm growth period, from initial colonization (2.5 days) to mature biofilm (18–25 days). (b) Evolution of the vertical profile of EPS in the biosedimentary beds. Polysaccharide content in the bound-EPS is presented with depth. Error bars are standard deviations between three replicates.

In this study, protein was present in the C-EPS during the entire growth period, while it only appeared in the B-EPS-fraction in surficial layers after 10 days of growth and in small amounts (less than 25 μg/g DW). It gradually became enriched in the surface as the biofilm matured eventually comprising nearly 15% of the total EPS [*Goto et al*., 2001; *Van Duyl et al*., 1999]. At the end of 25 days, the B-EPS protein was absent in the sublayers. A possible explanation was that the enrichment of the B-EPS protein usually lags behind polysaccharide as biofilms grow [*De Brouwer and Stal*, 2001; *Nielsen et al*., 1997]. In this study, the evolution of the vertical EPS polysaccharide profiles was related to the changes in sediment stability (Figure 3b) during the erosion process. However, this does not necessarily imply that proteins have no influence on biostabilization. Generally, the vertical profile of the B-EPS concentration (polysaccharides) showed an increase with time, but different vertical layers showed different patterns of development: EPS in the surficial layers accumulated more rapidly (with 2–3 times higher concentrations in the final profile) than the lower layers. By the end of the incubation period, the EPS was highly concentrated at the surface with the biofilm, and decayed sharply below the surface. Nevertheless, it showed that for noncohesive fine sand, EPS was not restricted to the bed surface, but could spread more deeply into sediment sublayers (Figure 3b). A relatively high EPS content ($>$60 μg/g DW) to a depth of 3–5 mm was found after 22 days. In addition, after the formation of a mature biofilm, the bound EPS in the sublayers continued to increase, implying that the depth profile may extend over time.

3.2. Sediment Particle Morphology

Scanning Electron Microscope (SEM) images show the morphology of the bed and accumulation of EPS at different stages of biofilm development (Figure 4). Images of surficial sediment samples were taken at the end of 2.5, 7.5, and 10 days while the vertical profile was analyzed after 22 days, with clean sediment as control. At the beginning of the incubation with bacteria, no visual changes were observed on the exposed clean sediment grain surfaces (i.e., 2.5 days). As bacterial growth advanced and EPS was produced, small

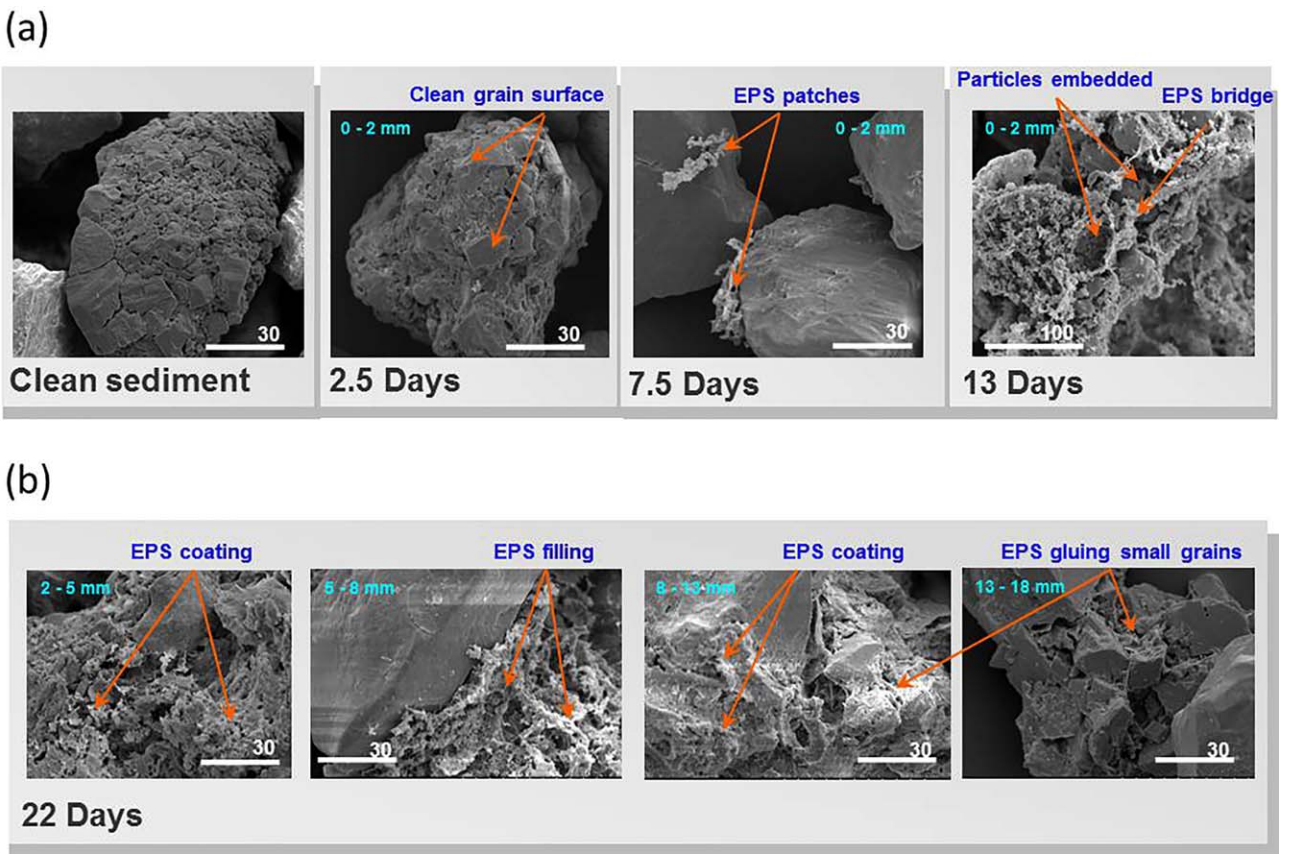

Figure 4. SEM images, illustrating sediment bed microstructure for sediment samples at the end of 2.5, 7.5, 10, and 22 days, with clean sediment as the control. Grain morphology of (a) the top layer is presented for 2.5, 7.5, and 10 days while (b) variations in vertical profile are shown for the biosedimentary system after 22 days. Scale bars are in micrometers (μm).

scattered localized patches of EPS were visualized attached to and covering the grain surfaces, but many clean faces still remained (7.5 days). EPS polysaccharides often show various degrees of branching, forming complex networks which add to the structural integrity of the EPS [*Pennisi*, 2002; *Wotton*, 2004]. As the biofilm gradually matured, most sediment grains were covered with EPS and bridging was present between individual particles (13 days). The vertical profile for biosedimentary systems indicated that biocohesion for the top 5 mm layers was clearly significant after 22 days. Almost all grain surfaces were embedded under EPS strands and webs. An EPS matrix connected separate particles together so that the overall bed roughness might be expected to decrease [*Paterson*, 1997]. Deeper into the bed (5–8 mm), grain surfaces were more exposed but EPS filling the pore spaces was still evident. In the bottom two layers, localized coating was observed but infilling and bridging was rare with connections only between smaller grains. Care must be taken in interpreting SEM images of polymeric material since the preparation of sediments for sampling can distort the natural matrix and so while the presence of EPS and its effects can be supported the exact confirmation of the material must be viewed with caution [*Perkins et al*., 2006].

3.3. Role of EPS on Sediment Erosion Process

3.3.1. Sediment Erosion Curves

Sediment erosion curves were generated from the time series of SSCs during the erosion experiments. A calculation has been performed on the eroded depth as a function of time to relate the EPS profile to the SSCs plot. This represents an equivalent depth of erosion, and requires several simplifying assumptions (discussed in supporting information Text S2). In this study, erosion processes were significantly mediated by growth-dependent biostabilization. Erosion threshold was defined as the point of initial erosion of the bed. For clean sediment, this was derived from a regression of SSC to applied bed-shear stress (full details of this method can be found in *Amos et al*. [2003]). Results showed that the critical shear stress for the clean sediment was 0.158 Pa ($r^2 = 0.924$). To facilitate comparison with other studies on sediment transport, the dimensionless threshold Shields parameter, θ_c, was used, which is defined as:

$$\theta = \frac{\tau_b}{(\rho_s - \rho) g D_{50}} \tag{1}$$

The threshold Shields parameter can be described as a function of the nondimensional grain size D_*, as follows [*van Rijn*, 1993]:

$$\begin{aligned} \theta_c &= \frac{\tau_{b_c}}{(\rho_s - \rho) g D_{50}} \\ &= 0.24 D_*^{-1} \qquad \text{for } 1 < D_* < 4 \end{aligned} \tag{2}$$

in which:

$$D_* = D_{50} \left(\frac{g\Delta}{\nu^2} \right)^{\frac{1}{3}} \tag{3}$$

with: τ_{b_c} = critical bed-shear stress; $\Delta = \frac{\rho_s}{\rho} - 1 = 1.65$; ν = kinematic viscosity of water = 1×10^{-6} m^2/s ($T = 20$°C), $g = 9.8$ m/s^2. For the very fine sand ($D_{50} = 108$ μm and $D_* = 2.73$) *tested in this study, the threshold for motion was 0.154 Pa, which is very close to the present experimental result of 0.158 Pa for the clean (control) sediment (<5%). Thresholds of motion obtained from the Shields diagram range from 0.154 to 5.28 Pa, with increasing of* D_*. Hence the sample used exhibits a low resistance to erosion in the absence of biofilm effects. However, a clear increase in the resistance of the surface to erosion was observed in the biosedimentary systems as the incubation period increasing (Figure 5). Result from the regression method showed that the critical shear stress increased to 0.189 Pa ($r^2 = 0.838$) for biosedimentary systems incubated for only 5 days. This is an increase of approximately 20% compared to the control (0.158 Pa in experiments or 0.154 Pa according to the Shields curve). For biosedimentary systems cultivated for 22 days, sediment was resistant to erosion up to a critical shear stress of 0.258 Pa, an increase of more than 60%. In addition, it should be noted that if the erosion is assessed using SSC, the onset of motion for the very fine sand as bed load could occur at a lower shear stress. Also with the increasing time of incubation it is worth noting the changes in the way that the incipient motion took place. When sediments are covered by biofilm, the entrainment process does not take place in a manner of a single rolling article, but occurs via biofilm failure and carpet-like erosion [*Haynes et al*., 2011]. *In other words, surface biofilm removal occurs in an "all-or-*

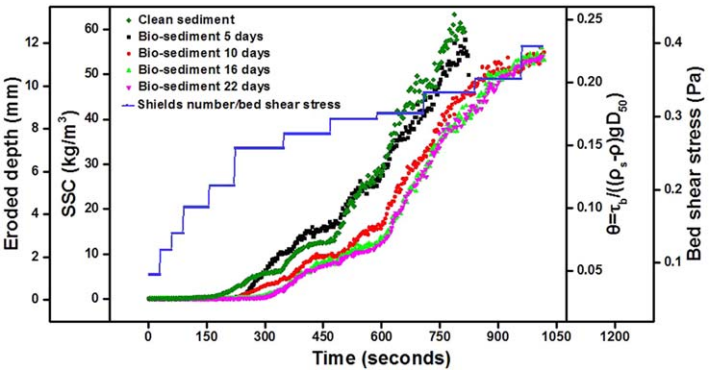

Figure 5. Erosion curves of biosedimentary systems (5, 10, 16, 22 days) and clean (control) sediment (22 days) represented by SSC values and eroded depth increasing with stepwise increment of shear stress during the entire erosion experiment.

nothing" fashion; the appearance of bed load before suspension is constrained to some extent in the biosediment system.

Various processes and properties of the sediment are mediated by biofilms, but probably one of the most important functional contributions of biofilms is stabilizing sediments, making them harder to be eroded [*Fagherazzi et al*., 2013]. This is achieved through a number of mechanisms: the formation of a tough layer or "skin" protecting underlying sediments; the smoothing of bed roughness; and the network effects of the secreted glue-like EPS [*Black et al*., 2002; *Paterson*, 1997]. Our results confirm that surface strength increases with time, with evidence that an upper limit or equilibrium (Figures 3 and 5) was reached by the end of the experiment.

It was also observed (Figure 5) that the effect of biostabilization was not limited to the sediment surface layers. The SSC produced from the erosion of deeper sediments suggested that biostabilization continued to mediate bed behavior after the loss of surficial sediment and biofilm. This is an important consideration for the modeling of sediment transport. It was clear that compared to the control, more time was needed for the biosedimentary beds to be eroded at a given applied bed-shear stress. However, the biological effects did not always increase sediment stability. Higher SSC was noted for the biosedimentary beds, as compared to the control, after 5 days of incubation when the EPS content was still relatively low (Figure 5). Although the erosion of sediments is a very stochastic process, the difference observed here goes beyond the natural variation between experiments (supporting information Figure S4). This suggests that once the initial protective effect of an incipient biofilm is removed, the excess stress produces more rapid erosion of the bed layers immediately beneath the surface. Analyses of the stratified EPS content provide further insight into this phenomenon. EPS can be classified into two main fractions: the C-EPS which are soluble in water, and the B-EPS that are tightly attached to the cell wall. EPS contents in the sublayer (2–5 mm) occurred as both colloidal and the bound forms of EPS. During the initial week of growth, there was a low level of B-EPS. As far as sediment properties are concerned, the C-EPS may not be such an effective stabilizing factor as B-EPS that can fill pore space and link sediment particles reducing erodibility [*Lubarsky et al*., 2010; *Orvain et al*., 2003, 2014; *Wingender et al*., 1999]. C-EPS help retain water in the sediment [*Perkins et al*., 2004] and consequently, during the early stage of development, high-water content as opposed to binding effects influences the erosion process. This has a negative influence on bed consolidation [*Wang et al*., 2015], hence decreasing the bed strength and sediment stability compared to the control. As the biofilm develops, binding effects from greater levels of B-EPS gradually counter-balance water content effects, thus leading to the higher biostabilization exhibited in the sublayer in the subsequent erosion phases (Figure 6).

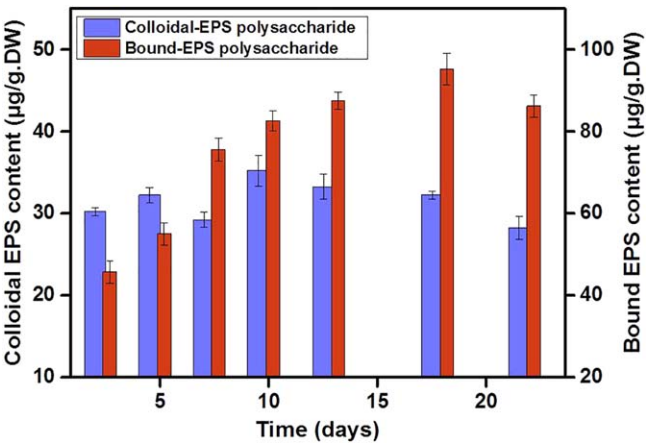

Figure 6. EPS contents of colloidal and bound EPS (polysaccharide) in the sublayer (2–5 mm) at different growth stages. Error bars are standard deviations for three replicates.

3.3.2. EPS Modified Erosion Patterns

Erosion rate per unit area of sediment bed is regarded as a robust measure of sediment stability and can be used to predict the SSC for an applied bed-shear stress [*Amos et al*., 2010]. Through analysis of the erosion rates and erosion patterns, the changes in the behavior of biosedimentary beds can be described. In the enclosed chambers, such as used in this study, the rate of erosion, E, is defined as:

$$E_{(t)} = \frac{(C_{t+\Delta t} - C_t)V}{\alpha \Delta t} \tag{4}$$

where C_t represents *SSC* at time t, V is the volume of water under consideration (0.0129 m^3), and α is the bed area (0.0483 m^2). The time series of erosion rates for each erosion curve: clean sediment at 22 days, biosedimentary systems at 5, 10, 16, 22 days are given (Figure 7). This is considered in the context of the "erosion types" proposed by Amos et al. [*Amos et al*., 1992, 1997]. According to this classification, Type Ia erosion is a surface phenomenon representing the removal of a thin organic "fluff" layer, which is often observed in nature at low current speeds when the bed initially floods in the tidal cycle. Type I erosion, the more dominant form, is characterized by an erosion rate that decays asymptotically with time, and is observed after Type I a. With increasing applied shear stress, Type II erosion occurs, which is represented by a constant erosion rate due to mass failure of the bed. The type of erosion reflects the nature of the sediment profile. This classification highlights how erosion rates changes with bed and flow conditions and incremental increases of shear stress.

The duration of the period before the onset of erosion and hence the critical shear stress for sediment surface erosion increased with time until 16/22 days (Figure 5). However, as the incubation period for the bacterial systems increased, a limit was reached for the time (and shear stress) required to initiate surface erosion. Minimal differences were then observed between the biosedimentary systems after 16 and 22 days, demonstrating that biostabilization reached (or approached) a stable equilibrium state after 2 weeks of incubation under these conditions. It should be noted that in a natural setting where applied shear stress, temperature, light, etc. vary temporally, different periods might be needed to reach equilibrium, and a true equilibrium may never be reached due to natural perturbations. It was noted that although the biosedimentary systems after 10, 16, and 22 days all failed at a similar shear stress (0.258 Pa), the increase in SSC (erosion rate) after the initial failure was further delayed as the incubation period increased. That is to say, the biological effects reduced the erosion rate (after exceeding the critical value) for a longer period. This demonstrated that even above the threshold conditions, sediment erosion was inhibited to an extent related to the incubation period. This suggests that natural erosion curves reflect different levels and depths of biological action, which advances traditional understanding of sediment erosion. Instead of acting on the surficial sediment directly, hydrodynamic forces first have to remove the organic covering of biofilm, which works as the first layer of protection. However, EPS can penetrate more deeply into the sediment and consequently reduces erosion rate for a finite period of time. With longer incubation periods and as the biofilm matures, this phenomenon becomes increasingly evident. After about 600s (eroded depth $\approx$3–4 mm, Figure 5), the erosion rates present similar slopes for all cases (Figure 7), both in trend and magnitude. This is reflected by the slope of the erosion curves (Figure 5) being parallel to each other as the erosion rates of the biosedimentary systems progressively increased to that of the control. The estimation of eroded depth also confirmed that the bed had been eroded down beyond the likely depth of EPS as derived from biochemical measurements. This reflects the reducing effect of EPS, as the upper sediments with high EPS contents were removed, exposing sediments with low concentrations of EPS with time and depth (Figure 3b).

The type of erosion did not change significantly between the clean sediment and biosediment system cultivated for 5 days. However, for the biosedimentary systems after 10, 16, and 22 days, clear differences were observed. Before the "Type I erosion" occurred, "no erosion" was followed by a period of low erosion rate events. The possible explanation for this could be the bed-age associated biostabilization. Only once the EPS matrix (the biofilm) was broken down and diffused into the water column, could the original sand grains be eroded. Hence, before sediment suspension, the biofilm was broken into small, loose, and poorly bound surface flocs and was eroded, representing a "Type Ia erosion" (Figure 7). After this loss of strength and integrity in the biofilm, the thin surface layer could be washed out within a very short space of time (e.g., $<$10 s). After losing the first layer of protection, the effect of the EPS coating and cohesion between sediment particles was still significant. This reflects the influence of EPS below the surface, which continued

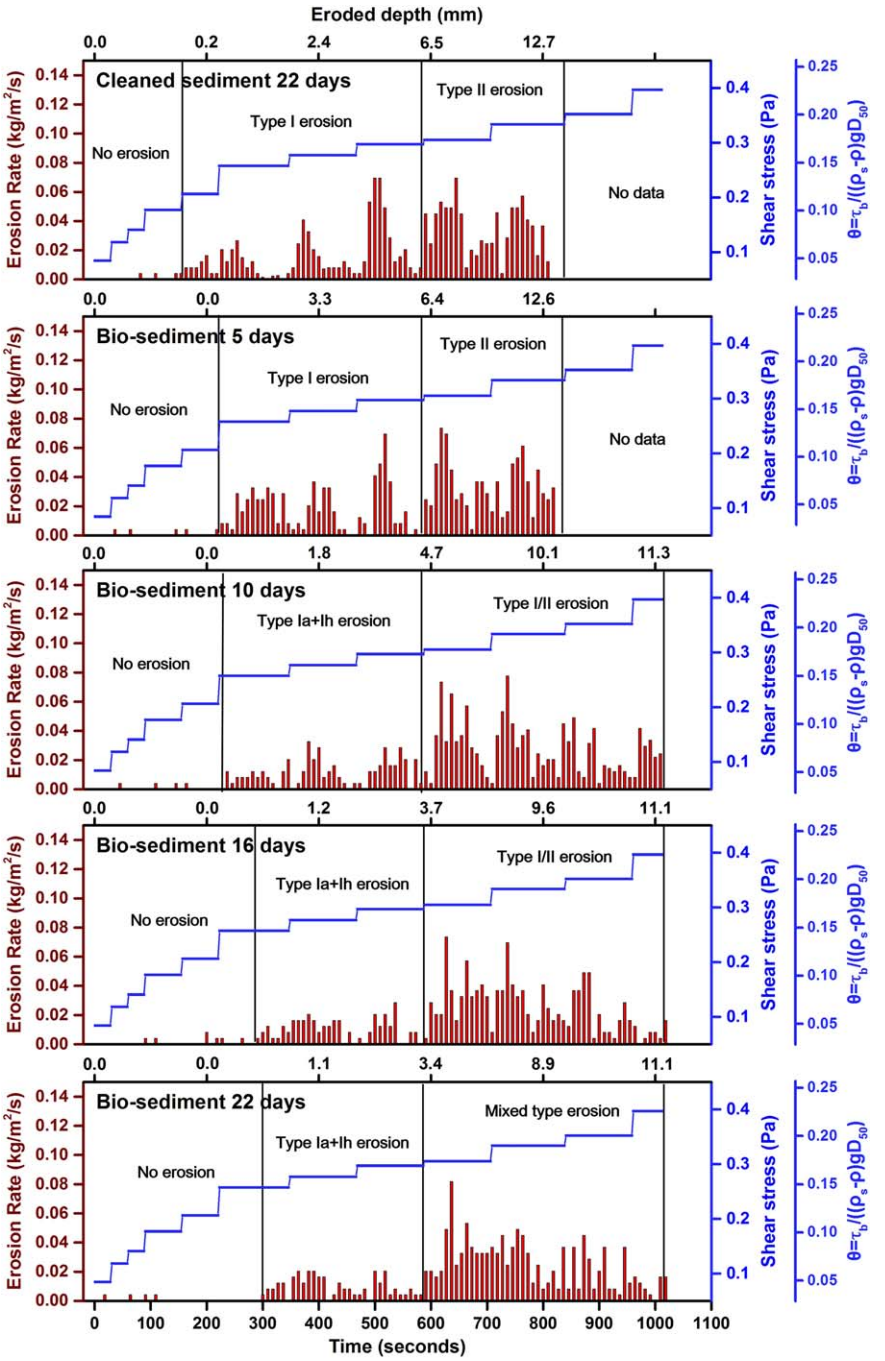

Figure 7. Time series of erosion rates and applied shear stress (and nondimensional Shields number) for biosediments after 5, 10, 16, 22 days and using clean sediment (control) after 22 days consolidation. Details of the erosion type are given in the text.

to act as a biostabilizer affecting the erosion rate of this lower bed material. This is represented by the difference in the gradient of the erosion profiles (Figure 3). EPS was present in relatively high contents within the upper layers (~3–5 mm for biosedimentary systems from 10 days to 22 days, respectively, Figure 3b). This effect has rarely been documented, but is an important aspect of biogenic stabilization. During this stage, resuspended sediment was mixed with organic matter, and can no longer be considered to be a "surface phenomenon." Therefore, another type of erosion that might be described as "hindered erosion" or "Type Ih" is suggested to characterize the process in the subsurface layers (eroded depth ~3–4 mm, Figure 7). Type Ih erosion is therefore expressed as the case where similar erosion profiles to Type I occur but particle movement is

hindered by organic material at greater depth once the surface stablization by the biofilm has been removed. The extent of the biological influence can be represented by a depth effect (DE) that represents the behavior of the control system (Type I) minus the erosion rate as influenced by EPS (Type Ih) as below:

$$\mathrm{DE} = \text{control rate (Type I)} - \text{hindered erosion (Type Ih)}$$

For biosedimentary systems, there was no clear boundary to separate Types I and II erosion. As a result, a transitional or mixed erosion type was found, where both consolidation and biocohesion contributed to the bed strength. It should be noted that the threshold for a fully Type II erosion was not always achieved by the end of the experiment for the more mature samples (bottom two plots in Figure 7).

Biostabilization of mud usually exhibits an increasing critical shear stress due to high surficial levels of EPS and biofilms, which cover the sediment surface and provide an initial layer of protection. In contrast, for sand particles, the surface phenomenon is generally weak, but the pervasive distribution of low levels of EPS can still play an important role. In this respect, the delay in ripple formation found by *Malarkey et al*. [2015] and the delay in the increase in sediment concentrations and transport rates found in our study are similar. In addition, Malarkey et al. pointed out that with low background levels of EPS, the ripples eventually reverted to abiotic dimensions with the gradual winnowing of EPS from the profile. Similar results were obtained here, that the bed strength reverted back to the abiotic condition when eroded to a depth with low EPS content. Hence, for noncohesive fine sands, despite exhibiting low resistance to erosion, biostabilization can make sand behave in a similar manner to cohesive sediment.

3.4. Biosedimentary System: Transformation From Traditional Perspectives

Most existing studies on the sediment erosion process of noncohesive fine sand in traditional systems explain the mechanism of sediment behavior in the absence of microbial effects. Under a low applied shear stress, physical forces such as gravity contribute to keep the bed stable. Sediment erosion occurs only when the shear force exceeds the erosion threshold, leading to the movement of sediment particles. However, in biosedimentary systems, the same erosion processes are mediated by EPS associated biostabilization.

In biosedimentary systems, the biological effects differ with growth period and development of the microbial communities. The biological mediation of sediment process is clearly related to the time and spatial scales of coastal changes, from local (daily and tidal) variation to geological (decadal) events. Microphytobenthos are adapted to the condition and can form biofilms very rapidly [*Underwood and Paterson*, 2003]. However, permanent biofilms and microbial mats require a longer period of time and the cycle-variation of the spring-neap tidal modulation favors biofilm development [*Mariotti and Fagherazzi*, 2012]. The variations of the hydrodynamics associated with tidal cycle allows biofilm to grow more easily during neap tide (when current shear stress is relative low), thus increasing biostabilization and the ability to withstand the subsequent energetic spring tides or other disturbance (i.e., wave, storms). This modulation will aid long-term maintenance of EPS within the system, in a cycle of production, breakdown, and redistribution that drives the EPS suffusing the sedimentary environment [*Malarkey et al*., 2015]. A longer time scale of variation is the seasonal change, as microbial growth and its metabolism are adjusted by the seasonal effects (e.g., temperature, irradiance). In addition, the large scale of long-term changes such as sea level rise could drive the migration of suitable zones for biocolonization.

The influence of biostabilization can go far beyond the initial erosion process (Figure 8). After erosion, EPS supports aggregation and changes the floc characteristics of the entrained material so that sediment transportation and deposition is also affected. During deposition the biosedimentary complex changes, further enhance the binding forces [*Droppo*, 2001, 2004]. This has implications for sediment and coastal processes. Sedimentology and geomorphology have traditionally been considered as fields in which physical and chemical processes dominate. Even when biological processes have been recognized, for example, in tidal flats, the focus has been almost entirely on vegetation (e.g., salt marshes, mangroves) or sometimes, on macrobenthos (e.g., crabs). However, microbial communities are not passive bystanders as they suffuse all sedimentary environments on earth and have been part of this ecology since the advent of bacteria 4.2 billion years ago [*Dodd et al*., 2017]. They influence sediments, contributing to a wide range of sedimentary processes and thus exercise a formative influence on coastal evolution. Biosedimentary systems exhibit more complex characteristics than abiotic systems, and require different modeling methods as compared with those in traditional settings. For instance, the thresholds for the initiation of sediment movement and subsequent erosion rates are no

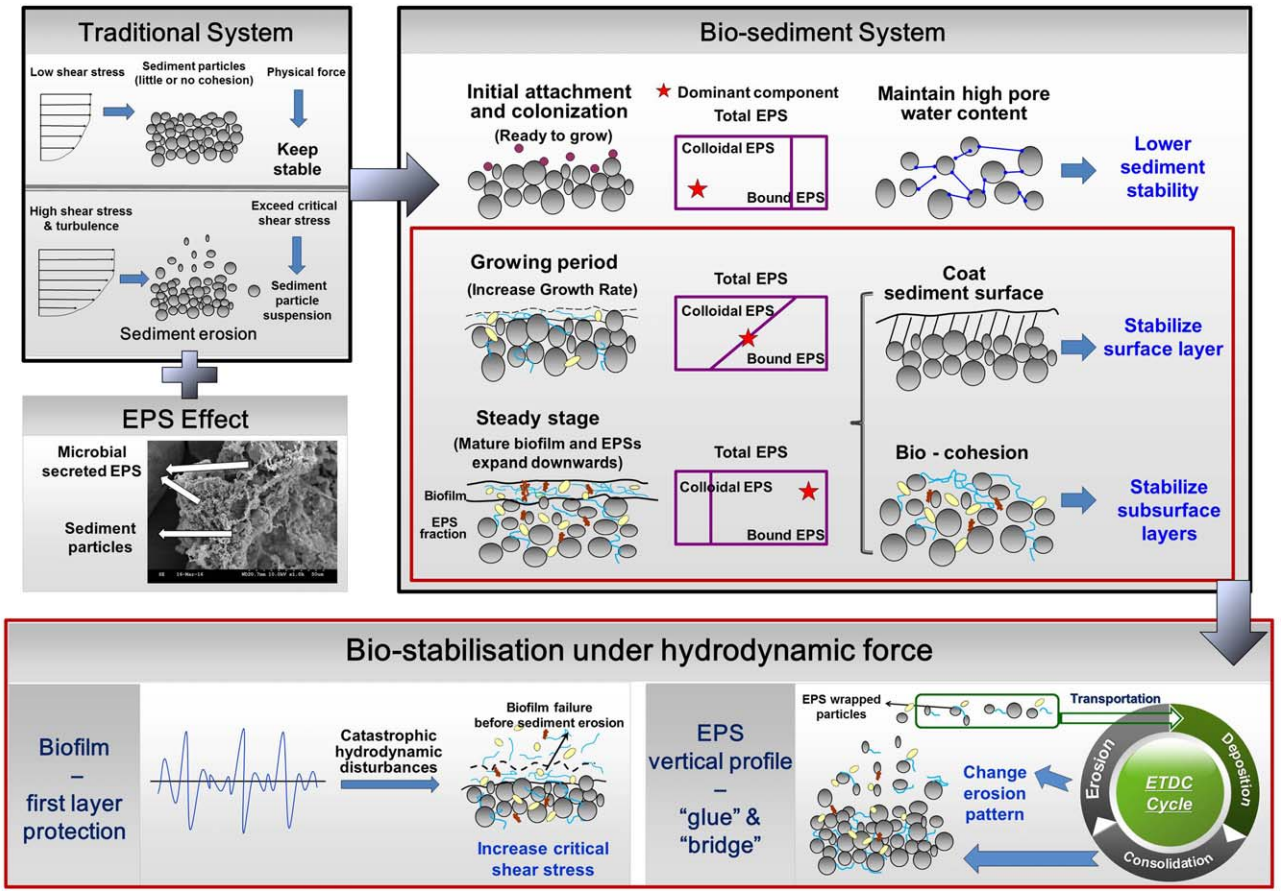

Figure 8. The conceptual model of how erosion processes can be mediated in biosedimentary systems compared to traditional abiotic systems. The performance of biostabilization in mediating sediment erosion processes varies for different growth stages (or different consolidation ages) due to the different extents and vertical distribution of EPS. After erosion, EPS-enveloped particles can influence the whole of the ETDC cycle, changing the transportation and deposition processes by forming bioflocs. Sediment consolidation with entrained EPS production sets up a new biosedimentary bed.

longer solely related to particle properties (e.g., particle size, the most widely used). From this point of view, it is easy to understand why data from field observations varies from predictions, usually appearing considerably strengthened. For example, instead of migrating constantly over time, sandy surface structures such as ripples can be preserved by biofilms [*Friend et al.*, 2008; *Noffke and Paterson*, 2008]. Our results indicate that the EPS mediation in sediment behavior vary with temporal variations in microbial growth, and reprofile the sediment stability during different stages of biofilm maturity.

4. Conclusions

This study shows that biophysical effects on sediment properties vary as the biofilm matures and this relate to the EPS distribution profile. At the beginning of the growth cycle, reductions in sediment stability were noted, likely due to changes in water content. Nevertheless, under favorable conditions, the noncohesive fine sand was stabilized by bound EPS. Importantly, this biostabilization affect was not only a "surface phenomenon" but also hindered subsequent erosion at greater depths in the bed. With increasing growth periods, bound EPS profiles in the vertical evolved. After 22 days of growth, the EPS content was concentrated at the surface as a biofilm, but had penetrated deeper into sublayers with a relatively high content (>60 μg/g DW) down to a depth of 3–4 mm, which then decayed sharply with depth. After the formation of a mature biofilm, the bound EPS in the sublayers still had the potential to extend to greater depths over time. Given the vertical distribution patterns of the EPS, the influence of biostabilization on bed strength varied with eroded depth. Consequently, the bed strength did not immediately revert to the noncohesive condition but progressively adjusted reflecting the depth profile of the EPS. This was termed "hindered erosion."

As erosion continued, erosion curves became parallel, indicating that the stability of the biosediment was progressively returned to that of the clean sediment.

Because of the protection of biofilms, the bed surface can withstand higher shear stress until biofilm failure. Moreover, sediment is not immediately suspended once the critical shear stress is reached but a gradual process of bed failure occurs as the organic layer is removed. It was noted that even though the biosedimentary systems, after 10, 16, 22 days, all began to erode at applied shear stresses of 0.258 Pa, the time taken for the initiation of sediment erosion after application of this stress was delayed as the growing period increased. More time was needed to induce the failure of the biofilm structure and to detach the biofilm before sediment erosion occurred. Hence, a time lag was found in the initiation of sediment erosion. With longer incubation periods, a more mature biofilm developed and this phenomenon became increasingly evident. Consequently, the biological effect not only increases the critical shear stress of the bed surface, but also enables it to withstand that threshold for a longer period of time.

In intertidal systems, where changes between "clean" sediment and EPS-influenced sediment occur in response to environmental variations (e.g., storms, tides, seasons, sea level rise), mediation in sediment stability may vary with different stages of the biostabilization succession. Therefore, the information from our study helps explain the natural variability with time and along a depth profile of bed properties. The large increase in both the critical shear stress and the erosion time relative to abiotic sand, as well as the large decrease in sediment transport, are potentially important for sediment transport modeling in the natural environment. Based on the above, our understanding of the sediment erosion process has advanced, and a conceptual framework has been put forward that transforms the traditional sediment system to an EPS-sediment system. It highlights the fact that EPS effects on bed erosion should be characterized as a bed-age associated depth-dependent parameter for inclusion in the next generation of sediment transport models. It is highlighted that the dynamic variability of biosediment has yet to be studied under the influences of multiple stressors in coastal environments, and this is the next stage of the journey.

Acknowledgments

This work was supported by the National Natural Science Foundation of China (NSFC, grants 51579072, 51620105005, 51379003, 41606104), the Fundamental Research Funds for the Central Universities of China (grants 2015B24814, 2016B00714, 2015B15814, 2015B25614), and the Jiangsu Provincial Policy Guidance Programme (BY2015002-05). Z. Zhou acknowledges the funding from Natural Science Foundation of Jiangsu Province (BK20160862). D. M. Paterson received funding from the MASTS pooling initiative (The Marine Alliance for Science and Technology for Scotland) and their support is gratefully acknowledged. MASTS is funded by the Scottish Funding Council (grant HR09011) and contributing institutions. Our thanks go to two laboratory assistants J. Xu and S. B. Yu, and to J. J. Zhou, N. Y. Zhang, B. B. Xu, C. Jin, and J. Wang for fruitful discussion on this work. We thank three anonymous reviewers and the associate editor for their constructive comments, which have helped to improve the manuscript. The data used to produce the results of this paper will be provided upon request.

References

Al-Ragum, A., M. Monge-Ganuzas, C. L. Amos, A. Cearreta, I. Townend, and E. Manca (2014), An evaluation of the Rouse theory for sand transport in the Oka estuary, Spain, *Cont. Shelf Res.*, *78*(3), 39–50.

American Public Health Association (APHA) (1998), *Standard Methods for the Examination of Water and* Wastewater, 20th ed., Am. Public Health Assoc./Am. Water Works Assoc./Water Environ. Fed., Washington, D. C.

Amos, C. L., J. Grant, G. R. Daborn, and K. Black (1992), Sea Carousel—A benthic, annular flume, *Estuarine Coastal Shelf Sci.*, *34*(6), 557–577, doi:10.1016/S0272-7714(05)80062-9.

Amos, C. L., T. Feeney, T. F. Sutherland, and J. L. Luternauer (1997), The stability of fine-grained sediments from the Fraser river delta, *Estuarine Coastal Shelf Sci.*, *45*(4), 507–524, doi:10.1006/ecss.1996.0193.

Amos, C. L., I. G. Droppo, E. A. Gomez, and T. P. Murphy (2003), The stability of a remediated bed in Hamilton Harbour, Lake Ontario, Canada, *Sedimentology*, *50*(1), 149–168, doi:10.1046/j.1365-3091.2003.00542.x.

Amos, C. L., G. Umgiesser, C. Ferrarin, C. E. L. Thompson, R. J. S. Whitehouse, T. F. Sutherland, and A. Bergamasco (2010), The erosion rates of cohesive sediments in Venice lagoon, Italy, *Cont. Shelf Res.*, *30*(8SI), 859–870, doi:10.1016/j.csr.2009.12.001.

Balke, T., P. M. J. Herman, and T. J. Bouma (2014), Critical transitions in disturbance-driven ecosystems: Identifying Windows of Opportunity for recovery, *J. Ecol.*, *102*(3), 700–708, doi:10.1111/1365-2745.12241.

Black, K. S., T. J. Tolhurst, D. M. Paterson, and S. E. Hagerthey (2002), Working with natural cohesive sediments, *J. Hydraul. Eng.*, *128*(1), 2–8, doi:10.1061/(ASCE)0733-9429(2002)128:1(2).

Craig, D., H. Fallowfield, and N. Cromar (2001), The effects of temperature and sediment characteristics on survival of *Escherichia coli* in recreational coastal water and sediment, *Environ. Health*, *1*(1), 43–50.

De Brouwer, J. F. C., and L. J. Stal (2001), Short-term dynamics in microphytobenthos distribution and associated extracellular carbohydrates in surface sediments of an intertidal mudflat, *Mar. Ecol. Prog. Ser.*, *218*, 33–44.

Dodd, M. S., D. Papineau, T. Grenne, J. F. Slack, M. Rittner, F. Pirajno, J. O Neil, and C. T. S. Little (2017), Evidence for early life in Earth's oldest hydrothermal vent precipitates, *Nature*, *543*, 60–64, doi:10.1038/nature21377.

Droppo, I. G. (2001), Rethinking what constitutes suspended sediment, *Hydrol. Processes*, *15*, 1551–1564.

Droppo, I. G. (2004), Structural controls on floc strength and transport, *Can. J. Civ. Eng.*, *31*, 569–578.

Droppo, I. G., S. N. Liss, D. Williams, T. Nelson, C. Jaskot, and B. Trapp (2009), Dynamic existence of waterborne pathogens within river sediment compartments. Implications for water quality regulatory affairs, *Environ. Sci. Technol.*, *43*(6), 1737–1743.

Fagherazzi, S., D. FitzGerald, R. Fulweiler, Z. Hughes, and P. Wiberg (2013), Ecogeomorphology of tidal flats, in *Treatise on Geomorphology*, edited by J. F. Shroder, pp. 201–220, Academic, San Diego, Calif.

Flemming, H. (2011), The perfect slime, *Colloids Surf. B*, *86*(2), 251–259, doi:10.1016/j.colsurfb.2011.04.025.

Friend, P. L., C. H. Lucas, P. M. Holligan, and M. B. Collins (2008), Microalgal mediation of ripple mobility, *Geobiology*, *6*(1), 70–82, doi:10.1111/j.1472-4669.2007.00108.x.

Gao, B., X. Zhu, C. Xu, Q. Yue, W. Li, and J. Wei (2008), Influence of extracellular polymeric substances on microbial activity and cell hydrophobicity in biofilms, *J. Chem. Technol. Biotechnol.*, *83*(3), 227–232, doi:10.1002/jctb.1792.

Garny, K., H. Horn, and T. R. Neu (2008), Interaction between biofilm development, structure and detachment in rotating annular reactors, *Bioprocess Biosyst. Eng.*, *31*(6), 619–629.

Gerbersdorf, S. U., T. Jancke, and B. Westrich (2005), Physico-chemical and biological sediment properties determining erosion resistance of contaminated riverine sediments—Temporal and vertical pattern at the Lauffen reservoir/River Neckar, Germany, *Limnologica—Ecol. Manage. Inland Waters*, *35*(3), 132–144, doi:10.1016/j.limno.2005.05.001.

Gerbersdorf, S. U., and S. Wieprecht (2015), Biostabilization of cohesive sediments: Revisiting the role of abiotic conditions, physiology and diversity of microbes, polymeric secretion, and biofilm architecture, *Geobiology*, *13*(1), 68–97, doi:10.1111/gbi.12115.

Goto, N., O. Mitamura, and H. Terai (2001), Biodegradation of photosynthetically produced extracellular organic carbon from intertidal benthic algae, *J. Exp. Mar. Biol. Ecol.*, *257*, 73–86.

Graba, M., S. Sauvage, F. Y. Moulin, G. Urrea, S. Sabater, and J. M. Sanchez-Pérez (2013), Interaction between local hydrodynamics and algal community in epilithic biofilm, *Water Res.*, *47*(7), 2153–2163, doi:10.1016/j.watres.2013.01.011.

Grant, J., and G. Gust (1987), Prediction of coastal sediment stability from photopigment content of mats of purple sulfur bacteria, *Nature*, *330*, 244–246.

Haag, I., U. Kern, and B. Westrich (2001), Erosion investigation and sediment quality measurements for a comprehensive risk assessment of contaminated aquatic sediments, *Sci. Total Environ.*, *266*(1–3), 249–257, doi:10.1016/S0048-9697(00)00753-1.

Hagadorn, J. W., and C. Mcdowell (2012), Microbial influence on erosion, grain transport and bedform genesis in sandy substrates under unidirectional flow, *Sedimentology*, *59*(3), 795–808, doi:10.1111/j.1365-3091.2011.01278.x.

Haynes, H., E. Vignaga, and W. T. Sloan (2011), *Biostabilisation of Coarse Sediment Using Cyanobacteria: Flow, Entrainment Threshold and Biomass, River, Coastal and Estuarine Morphodynamics: RCEM 2011*, Tsinghua Univ. Press, Beijing.

Le Hir, P., Y. Monbet, and F. Orvain (2007), Sediment erodability in sediment transport modelling: Can we account for biota effects? *Cont. Shelf Res.*, *27*(8), 1116–1142, doi:10.1016/j.csr.2005.11.016.

Li, T., R. Bai, and J. Liu (2008), Distribution and composition of extracellular polymeric substances in membrane-aerated biofilm, *J. Biotechnol.*, *135*(1), 52–57, doi:10.1016/j.jbiotec.2008.02.011.

Liang, Z., W. Li, S. Yang, and P. Du (2010), Extraction and structural characteristics of extracellular polymeric substances (EPS), pellets in autotrophic nitrifying biofilm and activated sludge, *Chemosphere*, *81*(5), 626–632, doi:10.1016/j.chemosphere.2010.03.043.

Lowry, O. H., N. J. Rosebrough, A. L. Farr, and R. J. Randall (1951), Protein measurement with the Folin phenol reagent, *J. Biol. Chem.*, *193*(1), 265–275.

Lubarsky, H. V., C. Hubas, M. Chocholek, F. Larson, W. Manz, D. M. Paterson, and S. U. Gerbersdorf (2010), The stabilisation potential of individual and mixed assemblages of natural bacteria and microalgae, *PLoS One*, *5*(11), e13794, doi:10.1371/journal.pone.0013794.

Malarkey, J. J., et al. (2015), The pervasive role of biological cohesion in bedform development, *Nat. Commun.*, *6*, 6257, doi:10.1038/ncomms7257.

Mariotti, G., and S. Fagherazzi (2012), Modeling the effect of tides and waves on benthic biofilms, *J. Geophys. Res. Biogeosci.*, *117*(G04010), doi: 10.1029/2012JG002064.

Nielsen, P. H., A. Jahn, and R. Palmgren (1997), Conceptual model for production and composition of exopolymers in biofilms, *Water Sci. Technol.*, *36*, 11–19.

Noffke, N., and D. Paterson (2008), Microbial interactions with physical sediment dynamics, and their significance for the interpretation of Earth's biological history, *Geobiology*, *6*(1), 1–4, doi:10.1111/j.1472-4669.2007.00132.x.

Orvain, F., R. Galois, C. Barnard, A. Sylvestre, G. Blanchard, and P. G. Sauriau (2003), Carbohydrate production in relation to microphytobenthic biofilm development: An integrated approach in a tidal mesocosm, *Microb. Ecol.*, *45*(3), 237–251, doi:10.1007/s00248-002-2027-7.

Orvain, F., M. De Crignis, K. Guizien, S. Lefebvre, C. Mallet, E. Takahashi, and C. Dupuy (2014), Tidal and seasonal effects on the short-term temporal patterns of bacteria, microphytobenthos and exopolymers in natural intertidal biofilms (Brouage, France), *J. Sea Res.*, *92*, 6–18, doi:10.1016/j.seares.2014.02.018.

Parsons, D. R., R. J. Schindler, J. A. Hope, J. Malarkey, J. H. Baas, and J. Peakall (2016), The role of bio-physical cohesion on subaqueous bedform size, *Geophys. Res. Lett.*, *43*(4), 1566–1573, doi:10.1002/2016GL067667.

Passarelli, C., F. Olivier, D. M. Paterson, T. Meziane, and C. Hubas (2014), Organisms as cooperative ecosystem engineers in intertidal flats, *J. Sea Res.*, *92*, 92–101, doi:10.1016/j.seares.2013.07.010.

Paterson, D. M. (1989), Short-term changes in the erodibility of intertidal cohesive sediments related to the migratory behavior of epipelic diatoms, *Limnol. Oceanogr.*, *34*(1), 223–234.

Paterson, D. M. (1997), Biological mediation of sediment erodibility: Ecology and physical dynamics, paper presented at Cohesive Sediments, in *4th Nearshore and Estuarine Cohesive Sediment Transport Conference INTERCOH'94*, edited by N. Burt, R. Parker and J. Watts, John Wiley and Sons, Wallingford, U. K.

Paterson, D. M., and G. R. Daborn (1991), Sediment stabilisation by biological action: Significance for coastal engineering, in *Developments in Coastal Engineering*, edited by D. H. Peregrine and J. H. Loveless, pp. 111–119, Univ. of Bristol Press, Bristol, U. K.

Paterson, D. M., and K. S. Black (1999), Water flow, sediment dynamics and benthic biology, in *Advances in Ecological Research*, edited by R. D and N. D, pp. 155–193, Oxford Univ. Press, Oxford, U. K.

Pennisi, E. (2002), Materials science—Biology reveals new ways to hold on tight, *Science*, *296*, 250–251.

Perkins, R. G., D. M. Paterson, H. Sun, J. Watson, and M. A. Player (2004), Extracellular polymeric substances: Quantification and use in erosion experiments, *Cont. Shelf Res.*, *24*(15), 1623–1635, doi:10.1016/j.csr.2004.06.001.

Perkins, R. G., I. R. Davidson, D. M. Paterson, H. Sun, J. Watson, and M. A. Player (2006), Low-temperature SEM imaging of polymer structure in engineered and natural sediments and the implications regarding stability, *Geoderma*, *134*(1–2), 48–55.

Pope, N. D., J. Widdows, and M. D. Brinsley (2006), Estimation of bed shear stress using the turbulent kinetic energy approach—A comparison of annular flume and field data, *Cont. Shelf Res.*, *26*(8), 959–970, doi:10.1016/j.csr.2006.02.010.

Raunkjaer, K., T. Hvitved-Jacobsen, and P. H. Nielsen (1994), Measurement of pools of protein, carbohydrate and lipid in domestic wastewater, *Water Res.*, *28*, 251–262.

Schindler, R. J., et al. (2015), Sticky stuff: Redefining bedform prediction in modern and ancient environments, *Geology*, *43*(5), 399–402, doi:10.1130/G36262.1.

Stapleton, K. R., and D. A. Huntley (1995), Seabed stress determinations using the inertial dissipation method and the turbulent kinetic energy method, *Earth Surf. Process Landforms*, *20*, 807–815.

Stone, M., B. G. Krishnappan, and M. B. Emelko (2008), The effect of bed age and shear stress on the particle morphology of eroded cohesive river sediment in an annular flume, *Water Res.*, *42*(15), 4179–4187, doi:10.1016/j.watres.2008.06.019.

Taylor, I. S., and D. M. Paterson (1998), Microspatial variation in carbohydrate concentrations with depth in the upper millimetres of intertidal cohesive sediments, *Estuarine Coastal Shelf Sci.*, *46*, 359–370.

Thompson, C. E. L., F. Couceiro, G. R. Fones, and C. L. Amos (2013), Shipboard measurements of sediment stability using a small annular flume-Core Mini Flume (CMF), *Limnol. Oceanogr. Methods*, *11*, 604–615, doi:10.4319/lom.2013.11.604.

Thomsen, L., and G. Gust (2000), Sediment erosion thresholds and characteristics of resuspended aggregates on the western European continental margin, *Deep Sea Res., Part I*, *47*(10), 1881–1897, doi:10.1016/S0967-0637(00)00003-0.

Tolhurst, T. J., E. C. Defew, J. F. C. D. Brouwer, K. Wolfstein, L. J. Stal, and D. M. Paterson (2006), Small-scale temporal and spatial variability in the erosion threshold and properties of cohesive intertidal sediments, *Cont. Shelf Res.*, *26*(3), 351–362.

Underwood, G., and D. M. Paterson (2003), The importance of extracellular carbohydrate production by marine epipelic diatoms., *Adv. Bot. Res.*, 40(05), 183–240.

Van Duyl, F. C., B. De Winder, A. J. Kop, and U. Wollenzien (1999), Tidal coupling between carbohydrate concentrations and bacterial activities in diatom-inhabited intertidal mudflats, Mar. Ecol. Prog. Ser., *191*, 19–32.

van Rijn, L. C. (1993), *Principles of Sediment Transport in Rivers, Estuaries and Coastal Seas*, Aqua Publications, Amsterdam, The Netherlands.

Vignaga, E., D. M. Sloan, X. Luo, H. Haynes, V. R. Phoenix, and W. T. Sloan (2013), Erosion of biofilm-bound fluvial sediments, *Nat. Geosci.*, *6*(9), 770–774, doi:10.1038/NGEO1891.

Volk, E. S. C. I., W. D. A. Furman, and R. Rosenzweig (2016), Biofilm effect on soil hydraulic properties: Experimental investigation using soil-grown real biofilm, *Water Resour. Res.*, *52*, 5813–5828, doi:10.1002/2016WR018866.

Wang, L., W. Zhu, J. Xie, L. Li, and C. Zhang (2015), Study of the shear strength of sediments in main sedimentation stages, *Mar. Georesour. Geotechnol.*, *33*(6), 556–566, doi:10.1080/1064119X.2015.1024902.

Wingender, J., T. Neu, and H. Flemming (1999), *Microbial Extracellular Polymeric Substances: Characterization, Structures and Function*, Springer, Berlin.

Wotton, R. S. (2004), The ubiquity and many roles of exopolymers (EPS) in aquatic systems, *Sci. Mar.*, *68*, 13–21.

Xu, F., J. Tao, Z. Zhou, G. Coco, and C. Zhang (2016), Mechanisms underlying the regional morphological differences between the northern and southern radial sand ridges along the Jiangsu Coast, China, *Mar. Geol.*, *371*, 1–17, doi:10.1016/j.margeo.2015.10.019.

Zhang, C. K., D. S. Zhang, J. L. Zhang, and Z. Wang (1999), Tidal current-induced formation—Storm-induced change—Tidal current-induced recovery—Interpretation of depositional dynamics of formation and evolution of radial sand ridges on the Yellow Sea seafloor, *Sci. China, Ser. D*, *42*(1), 1–12.

Zhang, Q., Z. Gong, C. Zhang, I. Townend, C. Jin, and H. Li (2016), Velocity and sediment surge: What do we see at times of very shallow water on intertidal mudflats? *Cont. Shelf Res.*, *113*, 10–20, doi:10.1016/j.csr.2015.12.003.

Zhou, Z., Q. Ye, and G. Coco (2016), A one-dimensional biomorphodynamic model of tidal flats: Sediment sorting, marsh distribution, and carbon accumulation under sea level rise, *Adv. Water Resour.*, *93*(B), 288–302, doi:10.1016/j.advwatres.2015.10.011.